

The use of normative models for verification to combined compression and bending in filled steel tubes with high strength concrete

Glaubert A. Miranda¹, Adenilcia F. G. Calenzani², Walnório G. Ferreira³

¹²³*Dept. of Civil Engineering, Federal University of Espírito Santo
Avenida Fernando Ferrari, 514, 29.075-910, ES/Goiabeiras. Vitória
glaubert.miranda@edu.ufes.br, adenilcia.calenzani@ufes.br, walnorio@gmail.com*

Abstract. Construction projects have demanded increasingly slender columns, consequently increasing the demand for efficient and economical solutions. One of the solutions adopted is the use of concrete and steel with high strengths and the use of optimized sections concrete-filled steel tubular columns, which has been widespread in European, American and Asian countries, however, in Brazil there is little application in construction. Combined bending and axial compression testing of composite columns can be carried out using simplified methods or analytical methods such as the deformation compatibility method. The draft revision of ABNT NBR 8800:2024 includes three simplified calculation models for combined bending and axial compression testing, limiting their application to concrete with a characteristic compressive strength of less than 50 MPa and steel with a yield strength profile of less than 450 MPa, as well as proposing polygonal lines for drawing the interaction curves. In this article, calculation models I and III from the draft revision of ABNT NBR 8800:2024 are compared with experimental results from the literature on specimen composite columns with filled circular tubular sections, classified as noncompact and slender. The specimen had concrete with a characteristic compressive strength in the range of 41 to 112.7 MPa. To do this, a computer tool was developed in MATLAB that plots the interaction curves of the ABNT NBR 8800:2024 revision project. The suitability and conservatism of the simplified methods when using high-strength concrete outside the normative range was verified.

Keywords: concrete-filled steel tubular columns, combined bending and axial compression, normative models, high strength concrete.

1 Introduction

In recent years, the field of structural engineering has witnessed a significant increase in demand for solutions that enable the construction of slimmer and more efficient columns. This trend is driven by the need to maximize usable space and reduce costs, without compromising the safety and structural capacity of buildings. One of the emerging approaches to meeting this demand is the use of concrete-filled steel tubular columns, which combine high-strength concrete with steel profiles. Although widely adopted in European, American and Asian countries, these systems are still relatively new in the context of Brazilian construction.

The current version of NBR 8800 [1] has two calculation models for checking compact section concrete-filled steel tubular columns subjected to combined bending and axial compression, as well as prescribing a reduction in the modulus of elasticity of the concrete to consider the effects of shrinkage and creep. However, in the case of concrete-filled steel tubular columns, the reduction in the modulus of elasticity of the concrete was dispensable. With the proposed 2024 revision, ABNT NBR 8800 [2] now has three calculation models for checking concrete-filled steel tubular columns subject to combined bending and axial compression. Model I is applicable to any type of section, whether compact, semi-compact or slender, model II is only applicable to compact sections and model III can be used for filled tubular columns with noncompact and slender sections. NBR 8800 [2] restricts

the use of slender sections to columns under pure compression. According to Lai and Varma [3], this is due to the lack of experimental results for combined bending and axial compression concrete-filled steel tubular columns. In addition, NBR8800 [2] is limited to normal strength concrete, i.e. concrete with a characteristic compressive strength within the range of 20 MPa to 50 MPa, so it is important to know the resistance capacity of concrete-filled steel tubular columns when using characteristic compressive strengths greater than 50 MPa. Calculation models I and III are based on the American standard, AISC 360-22 [4]. For the aforementioned normative calculation models, it is possible to represent their results graphically by polygons, as shown in Fig. 1.

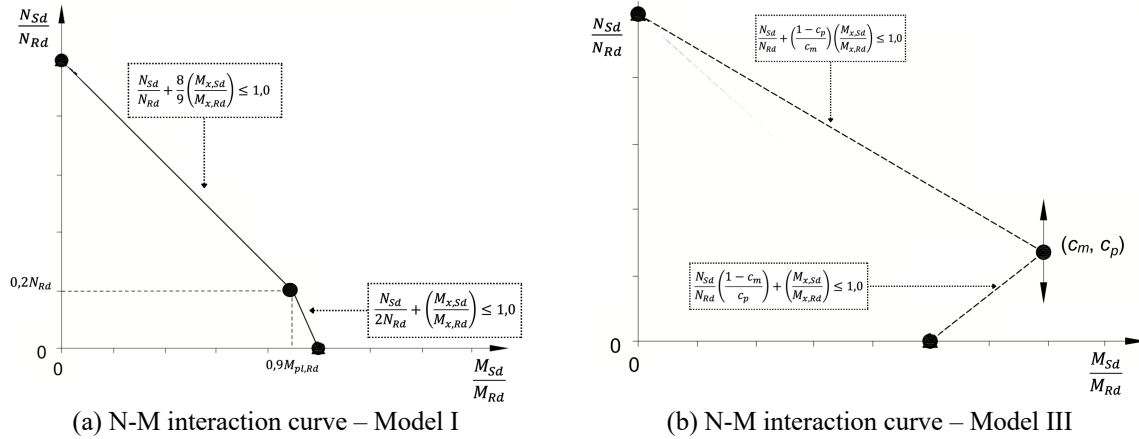


Figure 1. N-M interaction curve models I and III.

According to NBR 8800 [2], in order to calculate the bending resistance of noncompact section, it is first necessary to determine the moment of initiation of yielding, M_{eRd} , obtained from the stress distribution shown in fig. 2(a), where the position of the neutral axis of the cross-section is given by the distance a_y , and the stress varies linearly from the extreme top fiber to the height of $2a_y$, in the rest of the section, the stress distribution is constant and equal to the design yield stress of the steel, f_{yd} . Due to the circular geometry of the cross-section, the direct determination of the position of a_y is not trivial, and to solve this problem, the Symbolic Math Toolbox™ function of MATLAB [5] was used. The areas of the sectors of the cross-section, fig. 2(b), were calculated in MATLAB [5] using approximate geometric equations and then the forces resulting from the tension blocks were calculated, applying the balance of forces in the cross-section to determine the position of the neutral line, a_y , and the balance of moments to determine the moment of flow initiation, M_{eRd} . This computational method allows for a more detailed and efficient analysis of circular sections, increasing the applicability and precision of the design in accordance with current regulations.

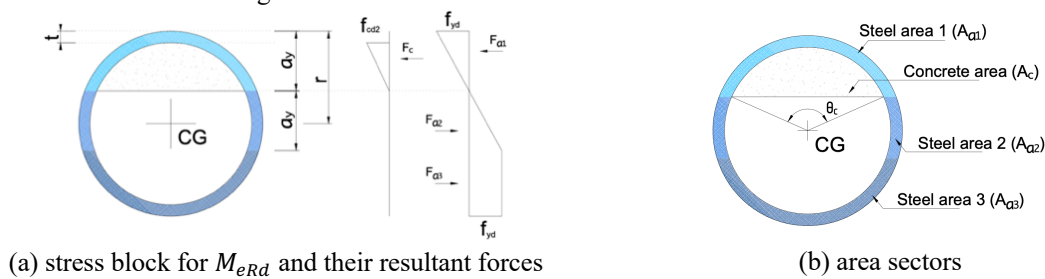


Figure 2. Stress blocks used to calculate the flexure strength of concrete-filled steel tube, M_{eRd} .

2 Combined bending and axial compression verification of concrete-filled tube according to NBR8800:2024

2.1 Normative approach

The calculation model I of NBR8800 [2] is like that of the AISC 360-22 standard [4], where the verification of resistance to axial force combined with the action of bending moments must be carried out in compliance with

the limitation of the interaction expressions prescribed by Eq. (1) and Eq. (2):

For $\frac{N_{Sd}}{N_{Rd}} \geq 0,2$:

$$\frac{N_{Sd}}{N_{Rd}} + \frac{8}{9} \left(\frac{M_{x,Sd}}{M_{x,Rd}} \right) \leq 1,0 \quad (1)$$

For $\frac{N_{Sd}}{N_{Rd}} < 0,2$:

$$\frac{N_{Sd}}{2N_{Rd}} + \left(\frac{M_{x,Sd}}{M_{x,Rd}} \right) \leq 1,0 \quad (2)$$

Based on Equation 1 and Equation 2, which are general (compound oblique bending), the answer is the bilinear graph shown in Fig.1 (compound straight bending). When the sum of the three terms of the first member of these expressions is less than 1.0, the point is located in the space between the surface and the origin 0, indicating a safe condition, but if the sum is greater than 1.0, the point is located in the space outside the region between the surface and the origin, indicating an unsafe situation, and in conditions where the sum is equal to 1.0, the point is located on the surface, still indicating a safe situation, but at the limit. Calculation model III, adapted from the AISC 360-22 standard [4], provides for the verification of resistance to axial force combined with the action of bending moments, complying with the limitations set out in Eq. (3) and Eq. (4):

For $\frac{N_{Sd}}{N_{Rd}} \geq c_p$;

$$\frac{N_{Sd}}{N_{Rd}} + \left(\frac{1 - c_p}{c_m} \right) \left(\frac{M_{x,Sd}}{M_{x,Rd}} \right) \leq 1,0 \quad (3)$$

For $\frac{N_{Sd}}{N_{Rd}} < c_p$;

$$\frac{N_{Sd}}{N_{Rd}} \left(\frac{1 - c_p}{c_m} \right) + \left(\frac{M_{x,Sd}}{M_{x,Rd}} \right) \leq 1,0 \quad (4)$$

Where c_p and c_m are the coefficients responsible for calibrating the combined bending and axial compression resistance calculated according to the type of section, for filled rectangular and circular tubular columns. Figure 1 illustrates the interaction curve for calculation model III, which represents Eq.3 and Eq.4 in graphical form, under the assumption of a bending moment in relation to one of the main axes. According to Lai and Varma [3] point C can be called the equilibrium point; it is responsible for improving the resistance of the composite section subjected to bending-compression

3 Computer tool

The concrete-filled steel tubular columns with a circular cross-section are more complex when it comes to determining the resistance to bending moments than concrete-filled steel tubular with a rectangular cross-section. This difficulty lies in the calculation of geometric properties such as the area and center of gravity of the compressed and tensioned regions, to determine the bending moment corresponding to the start of yielding of the composite section. In this work, we used geometric expressions to calculate the area and centroid of the circular sector A_{a1} , the circular crown sector, A_{a2} and the circular segment A_{a3} , (see Fig. 2(b)). To automate the verification of combined bending and axial compression in concrete-filled steel tubular columns, a computational program was developed using MATLAB [5], which plots simplified interaction curves based on NBR 8800 [2] standards. This tool addresses the calculation of concrete-filled steel tubular, without longitudinal reinforcement, doubly pinned at the ends, and with compact, noncompact, and slender cross-sections. The validation of the tool is performed through two numerical examples: the first example, taken from Araújo et al. [6], involves a compact section column, and the second example, manually solved by the authors, concerns a noncompact section column.

4 Results and discussions

4.1 Validation example

The first validation example, taken from Araújo et al. [6], is a compact concrete-filled steel tubular columns, as shown in Fig. 3, with a length of 4 m. The applied forces N_{sd} and M_{sd} are 5869.4 kN and 20871.60 kN, respectively. The concrete strength f_{ck} and steel yield strength f_y are 40 MPa and 350 MPa, respectively, with granite and gneiss aggregate. The second validation example, also depicted in Fig. 3, has the same diameter as the first example but with a wall thickness of 4 mm, resulting in a noncompact section.



Figure 3. Validation example

Araújo et al. [6] verified the column in Fig. 3(a) using NBR 8800 [1], while the authors employed the revised draft version of NBR 8800 [2]. In Table 1, predictions from NBR 8800 [1] and [2] are compared. The utilization ratio, i_a , is derived from the interaction equation of the models; thus, if i_a is less than one, the column meets safety requirements. It is evident that the normative revision results in a significant difference for combined bending and axial compression verification using calculation model II, impacting bending resistance substantially.

Tabela 1. The difference between the results of NBR8800 [1] and [2]

Índices	Modelo I			Modelo II		
	NBR 8800 [1]	NBR 8800 [2]	Diferença	NBR 8800 [1]	NBR 8800 [2]	Diferença
N_{sd}/N_{Rd}	0.6625	0.6632	0.10%	0.6518	0.6513	0.07%
M_{sd}/M_{Rd}	0.2641	0.2633	0.30%	0.2934	0.2925	0.30%
i_a	0.8973	0.8900	0.82%	0.9230	1.0600	12.92%

The second validation example was defined by reducing the thickness of the steel tube from the first example until the section became noncompact. The applied forces were also adjusted so that the combined bending and axial compression interaction equation would be satisfied, providing a utilization ratio less than one. Therefore, N_{sd} and M_{sd} are taken as 3100 kN and 3415.18 kN.m, respectively. The results obtained by the tool for the second validation example were compared with manually calculated results, and the tool proved to be reliable. From Figure 4, it is observed that calculation model III yielded the lowest utilization ratio among the calculation models specified in NBR 8800 [2].

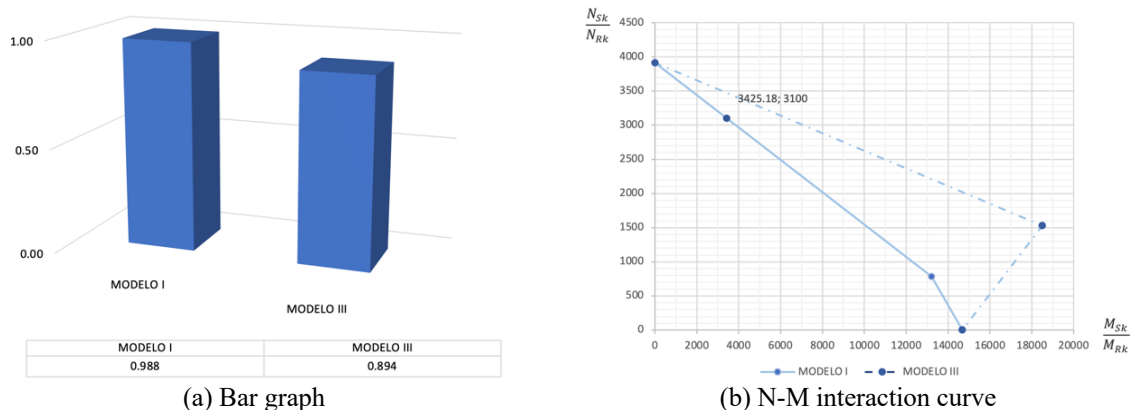


Figure 4. Results from the second validation example.

5 Analysis of combined bending and axial compression in noncompact sections

With the calculation tool properly calibrated, this study analyzed concrete-filled steel tubular columns of noncompact and slender sections. These columns were tested by O'Shea and Bridge [7], applying eccentric loading to specimens, and by Prion and Boehme [8], using a four-point loading scheme. The characteristics and properties of these columns are presented in Tab. 2, where it is noted that the characteristic strength of concrete varies from 41 MPa to 112.7 MPa.

Table 2. Geometric properties and applied forces

Reference	Specimen	L (mm)	D (mm)	t (mm)	f_y (MPa)	f_c (MPa)	P_{exp} (kN)	M_{exp} (kN.m)
O'Shea and Bridge [7]	S12E250A	663.5	190	1.13	185.7	41	1229.0	10.5
	S10E250A	662	190	0.86	210.7	41	1219.0	9.0
	S12E150A	664	190	1.13	185.7	41	1023	19.3
	S10E150A	663	190	0.86	210.7	41	1017	14.1
	S12E210B	662	190	1.13	185.7	113.9	2438	20.7
	S10E280B	665.5	190	0.86	210.7	74.4	1910	16.4
	S16E180A	66.35	190	1.52	306.1	80.2	1925	27.5
	S10E180B	665	190	0.86	210.7	74.7	1532	27.4
	S16E110B	660.5	190	1.52	306.1	112.7	2420	31.2
Prion and Boehme [8]	S12E110B	662	190	1.13	185.7	112.7	1925	32.9
	BP11	2120	152	1.70	328	92	470	29.7
	BP12	2120	152	1.70	328	92	570	32.1
	BP13	2120	152	1.70	328	92	670	28.5
	BP14	2120	152	1.70	328	92	820	29.2
	BP15	2120	152	1.70	328	92	970	30.5
	BP17	2120	152	1.70	328	92	270	30.1
	BP18	2120	152	1.70	328	92	270	30.8
	BP19	2120	152	1.70	328	92	670	34.8

For axial loading, the ultimate axial force from the test P_{exp} was considered, and the computational tool returned the maximum bending moment that, together with the axial force, satisfies the interaction expression. Table 3 presents the maximum moment results for the O'Shea and Bridge [7] specimen, obtained using Equations (1), (2), and (3), with weighting factors set to one and using granite and gneiss aggregates. Maximum moment values were not provided for specimen S10E250A, S12E150A, S12E210B, S10E280B, and S16E180A because the ratio between experimental axial load and the resistant axial load per the standard exceeds unity, thereby surpassing normative limits for calculation models. Calculation model I underestimated the combined bending and axial compression resistance capacity, as the ratio $M_{m\acute{a}x}/M_{exp}$ was consistently less than 0.2. In contrast, calculation model III provided a better prediction, albeit still very conservative, with $M_{m\acute{a}x}/M_{exp}$ ratios ranging from 0.034 to 0.942.

Table 3. O'Shea and Bridge [5] and Author results

Specimen	P_{exp} (kN)	M_{exp} (kN.m)	Resistance capacity NBR 8800 [2]		Maximum moment obtained from the interaction equation		Comparison: Standard versus Experiment	
			N_{Rk} (kN)	M_{Rk} (kN.m)	Modelo I $M_{m\acute{a}x}$ (kN.m)	Modelo III $M_{m\acute{a}x}$ (kN.m)	Modelo I $M_{m\acute{a}x}/M_{exp}$	Modelo III $M_{m\acute{a}x}/M_{exp}$
S12E250A	2438.00	20.70	3172	12.84	3.342	19.50	0.161	0.942
S10E250A	1229.00	10.50	1224	10.49	-	-	-	-
S12E150A	1219.00	9.00	903	8.62	-	-	-	-
S10E150A	1023.00	19.30	1224	10.49	1.939	8.46	0.100	0.438
S12E210B	1017.00	14.10	903	8.62	-	-	-	-
S10E280B	1910.00	16.40	1554	9.39	-	-	-	-
S16E180A	1925.00	27.50	1817	21.98	-	-	-	-
S10E180B	1532.00	27.40	1560	9.40	0.190	2.54	0.007	0.093
S16E110B	2420.00	31.20	2442	20.05	0.203	1.08	0.007	0.034
S12E110B	1925.00	32.90	3140	10.74	4.676	15.20	0.142	0.462

The specimen tested by Prion and Boehme [8] were identical, and the authors varied the applied forces until collapse occurred. The results of the maximum moment obtained by the computational tool are presented in Table 4, where it is observed that once again, model III shows more consistent results with experimental findings (0.659 ≤ $M_{m\acute{a}x}/M_{exp}$ ≤ 0.947), demonstrating closer agreement compared to model I (0.288 ≤ $M_{m\acute{a}x}/M_{exp}$ ≤ 0.527), which exhibited an average discrepancy of 58%. These tests underscored the importance of calibrating calculation models, particularly considering concrete strength properties and the effects of shrinkage and creep under variable loading conditions. It is concluded that more comprehensive studies should be conducted to enable the application of calculation model III in concrete-filled steel tubular columns with high-strength concrete, exceeding 50 MPa in compressive strength. Calculation model I did not prove to be a satisfactory alternative, as expected, since its interaction curve is the same as that used for purely steel columns, leading to overly conservative results composite columns.

Table 4. Prion and Boehme [6] and Author results

Specimen	Resistance capacity NBR 8800 [2]				Maximum moment obtained from the interaction equation		Comparison: Standard <i>versus</i> Experiment	
	P_{exp} (kN)	M_{exp} (kN.m)	N_{Rk} (kN)	M_{Rk} (kN.m)	Modelo I $M_{m\acute{a}x}$ (kN.m)	Modelo III $M_{m\acute{a}x}$ (kN.m)	Modelo I $M_{m\acute{a}x}/M_{exp}$	Modelo III $M_{m\acute{a}x}/M_{exp}$
BP11	470	29.7	1779	17.16	14.20	22.63	0.478	0.762
BP12	570	32.1	1779	17.16	13.11	23.79	0.409	0.741
BP13	670	28.5	1779	17.16	12.03	24.95	0.422	0.876
BP14	820	29.2	1779	17.16	10.40	26.70	0.369	0.947
BP15	970	30.5	1779	17.16	8.77	28.45	0.288	0.933
BP17	270	30.1	1779	17.16	15.85	20.30	0.527	0.674
BP18	270	30.8	1779	17.16	15.85	20.30	0.515	0.659
BP19	670	34.8	1779	17.16	12.03	24.95	0.346	0.717

With the data and results extracted from Tables 2, 3, and 4, the MATLAB tool develops interaction curves for both calculation models, as shown in Figures 5 to 15. The more conservative nature of model I is evident, as its curve is contained within the area delineated by the model III curve.

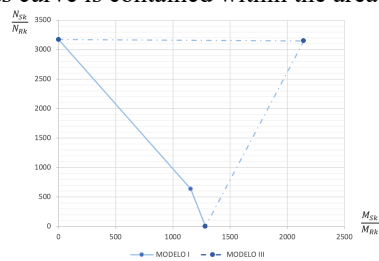


Figure 5 M-N specimen S12E210B

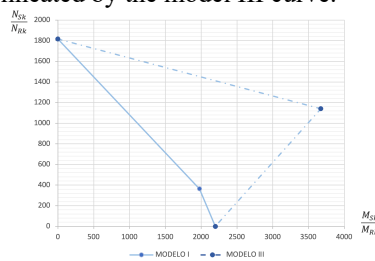


Figure 8 M-N da amostra S16E180A

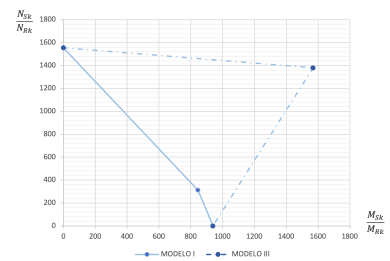


Figure 11 M-N da amostra S10E280B

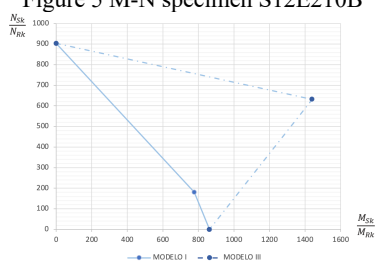


Figure 6 M-N da amostra S10E250A

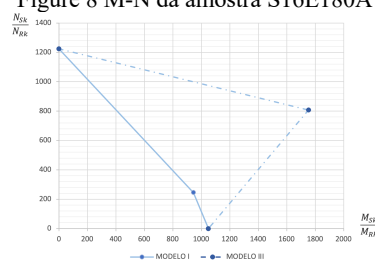


Figure 9 M-N specimen S12E250A

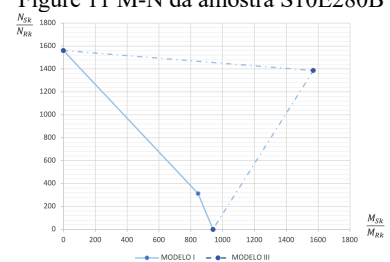


Figure 12 M-N da amostra S10E180B

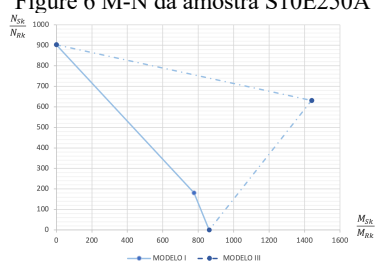


Figure 7 M-N specimen S10E150A

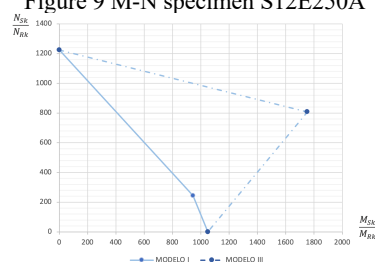


Figure 10 M-N da amostra S12E150A

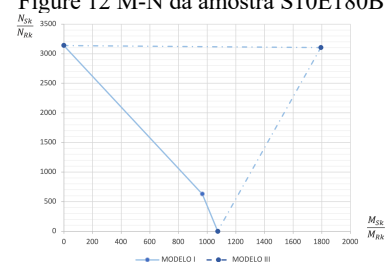


Figure 13 M-N da amostra S12E110B

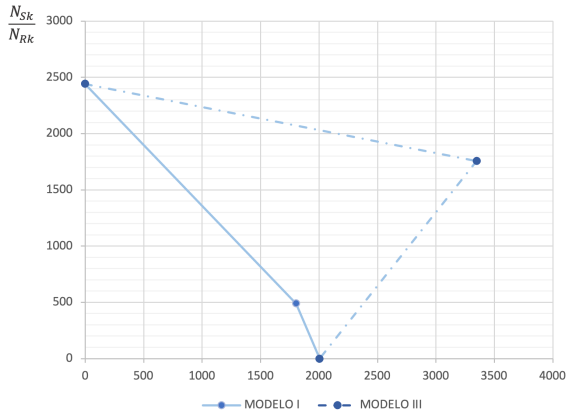


Figure 14 M-N da amostra S16E110B

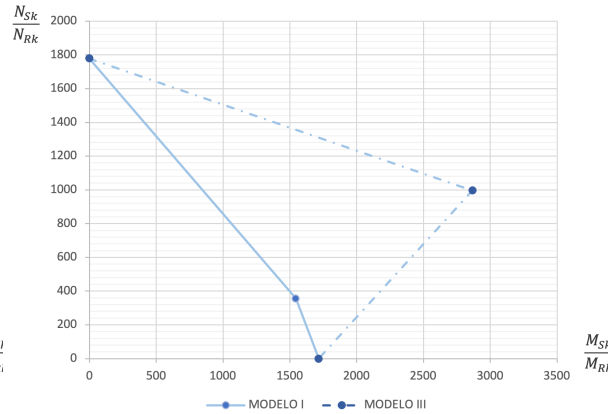


Figure 15 M-N da amostra BP11 a BP19

6 Conclusion

In this study, a computational tool was developed to verify combined bending and axial compression in concrete-filled steel tubular columns of compact, noncompact, and slender circular sections. The computational tool was validated using numerical examples that allowed for a comparison between calculation models I and II of the Brazilian standard ABNT NBR 8800. Following validation, an analysis of columns with concrete strengths exceeding 50 MPa was conducted using specimen tested in the literature. It was confirmed that calculation models I and III provide conservative approximations. For both noncompact and slender sections, calculation model III of NBR 8800, recently added in the 2023 version, proved to be less conservative than model I. This can be observed from the interaction curves, where the model III curve of NBR 8800 has a larger enclosed area. However, more comprehensive studies are needed to enable the application of calculation model III in concrete-filled steel tubular columns with concrete having compressive strength exceeding 50 MPa.

References

- [1] ASSOCIAÇÃO BRASILEIRA DE NORMAS TÉCNICAS (2008), NBR 8800:2008. Projeto e execução de estruturas de aço e de estruturas mistas aço-concreto de edifícios. Rio de Janeiro.
- [2] ASSOCIAÇÃO BRASILEIRA DE NORMAS TÉCNICAS (2024), NBR 8800:2008. Projeto e execução de estruturas de aço e de estruturas mistas aço-concreto de edifícios: Projeto de revisão 2024. Rio de Janeiro.
- [3] Lai Z, Varma AH. Noncompact and slender circular CFT members: experimental database, analysis, and design. *J Constr Steel Res* 2014.
- [4] AISC. 360-05. Specification for structural steel buildings. Chicago, IL, USA: AISC; 2005.
- [5] MATLAB M. The language of technical computing. The MathWorks, Inc, 2023. Disponível em: <http://www.mathworks.com>.
- [6] Araújo, A. H. M., Sarmanho A. M., Batista E. M., Requena J. A. V., Fakury R. H., Pimenta R. J. Projeto de Estruturas de Edificações com Perfis Tubulares de Aço. Belo Horizonte: Rona Editora LTDA, 2016.
- [7] O'Shea MD, Bridge RQ. Design of circular thin-walled concrete filled steel tubes. *J Struct Eng* 2000;126:1295–303.
- [8] Prion HGL, Boehme J. Beam-column behaviour of steel tubes filled with high strength concrete. *Can J Civ Eng* 1994;21:207–13.